DESIGN AND ANALYSIS OF TECHNOLOGIES FOR LOAD CONTROL

(ENTWICKLUNG UND ANALYSE VON TECHNOLOGIEN ZUR LASTABMINDERUNG)

Wolf R. Krüger[1], Kjell Bramsiepe, David Quero Martin, Andreas Goerttler, Ruben Seidler, Sascha Dähne, Sven C. Künnecke, Daniel Kiehn, Thiemo Kier, Christian Wallace

Deutsches Zentrum für Luft- und Raumfahrt (DLR)
[1] Institut für Aeroelastik, Bunsenstr. 10, 37073 Göttingen, Wolf.Krueger@DLR.de

Summary

In the DLR project "Optimally Load-Adaptive Aircraft" (oLAF), the use of methods for reducing flight loads on commercial aircraft has been investigated in detail. In a dedicated work package, specific technologies for load reduction have been developed and made available to the other work packages of the project, i.e. aircraft design, wind tunnel tests, and MDO processes. The paper provides an overview of the approaches taken and the results achieved in this work package.

1. BACKGROUND: FLIGHT LOAD ALLEVIATION IN AIRCRAFT DESIGN

Passive and active flight load alleviation is an important contribution towards lighter wing structures and wings of higher aspect ratios, both important measures to increase the efficiency of transport aircraft. In the DLR project oLAF (Optimally Load-Adaptive Aircraft), strategies for active and passive load alleviation have been developed and validated. In the project, different lines of investigation were followed in parallel – first, a reference configuration of a long-range aircraft has been designed on a preliminary design basis, and both aerodynamics and structure of the wing were further optimized using coupled CFD- and finite-element-based design methods. Second, various aspects of load control technologies have been studied independently, and the results were applied using the design process of the reference aircraft. Third, a closer look has been taken at the aerodynamics of spoilers and control surfaces. Finally, high-fidelity methods have been employed for a further development of MDO aircraft design processes.

In a dedicated work package of oLAF, innovative methods for the reduction of flight loads on commercial aircraft have been developed and their performance was evaluated. The following approaches have been pursued: First, the application of non-linear materials for wing design has been evaluated, globally assessing the potential of such an approach for load reduction. A specific implementation of that approach can be the exploitation of non-linear buckling behaviour of the wing skin. Second, a so-called morphing spoiler has been developed as a control device combining the properties of a classical spoiler and a shock control bump (also to be used for load control) in a single unit. Third, active control has been further developed, both in the form of robust feed-back control, and on the characterization of lidar behaviour, which is a crucial technological component for feed-forward control. In addition, numerical approaches have been further developed, in the form of reduced models for mini flaps and spoilers, and CFD-based reduced models for classical control surfaces. Finally, CFD-based fast models to be used for load control and flutter control have been developed.

2. REFERENCE AIRCRAFT

For the investigation of the potential of aggressive load alleviation a long-range aircraft configuration is developed and taken as a reference. In a first loop, the aircraft is designed assuming classical load alleviation approaches, especially manoeuvre load alleviation, using the standard control surfaces (the so-called “baseline design”). In a second loop, roughly half way through the project, selected additional load alleviation technologies are implemented on the aircraft and the potential for load reduction of the respective technologies is evaluated. The sizing of the aircraft structure is now repeated with a set of newly determined loads, thus assessing the potential of the load alleviation technologies for a wing mass reduction (“final design”).

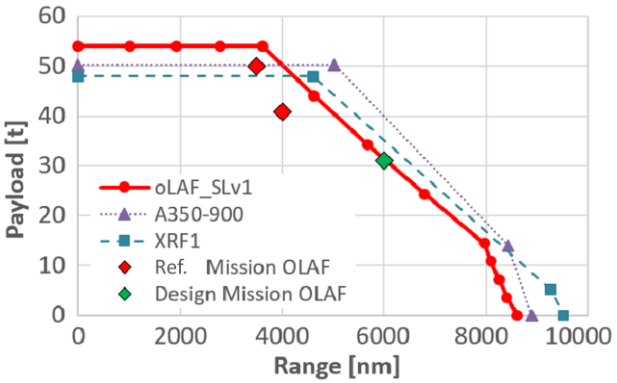

Figure 1. Payload-range diagram for the oLAF configuration

The reference aircraft in oLAF is a wide-body long-range configuration, closer described in [1], [2], [3]. Top level aircraft requirements are an OEM of 118 t, an MTOM of 220 t, a maximum payload of 54 t and a flight Mach number MMO of 0.86. The wing span of the initial configuration is 57.7 m, with an aspect ratio of roughly 10.

The design parameters are shown in the payload-range-diagram in Figure 1, taken from [1], compared to parameters of the Airbus research model XRF1, a long-range wide body transport aircraft developed by Airbus as part of the eXternal Research Forum, and publicly available data of the commercial Airbus A350-900.

doi: 10.25967/630076

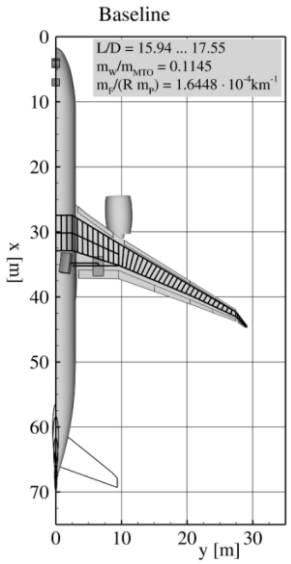

Figure 2. Planform of reference aircraft

For the conceptual design, the aircraft design tool openAD is used. The process consists of a single loop converging the maximum take-off mass and fuel mass. OpenAD is used to obtain the main geometrical parameters for the wing, fuselage, and tail planes, an initial mass-breakdown, a costs estimation and a simplified aerodynamic performance map. The tool has the additional functionality to generate a CPACS file [4] which is the basis for aircraft data exchange in the project.

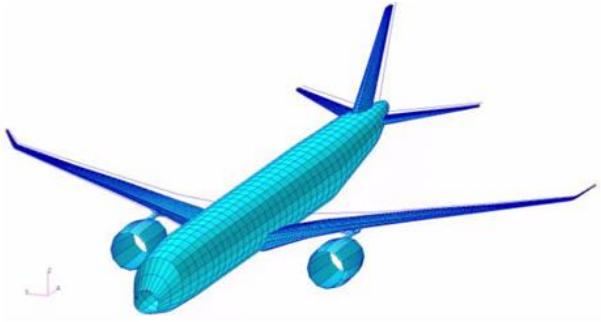

Figure 3. oLAF reference configuration: GFEM model

Based on the result of the overall aircraft design, parametric models for the aero-structural wing optimization are built. This design step consists of an optimization process which is based on using CFD and finite element analysis methods, with requirements from a multi-mission analysis. The conceptual design is enhanced by introducing more aerodynamic performance driving profiles and twist distribution based on previous wing planform optimization results [2]. As a further result, the wing planform of the oLAF configuration was the input for the wind tunnel model wing used to demonstrate active load alleviation approaches in oLAF, see Section 4 below.

In a subsequent analysis, the aeroelastic design and assessment is performed, including an extensive flight load analysis campaign of the flexible aircraft and a structural optimization of the wing structures taking loads as well as aeroelastic requirements like sufficient control surface efficiency into account [2]. The analyses are performed using a global finite element model (the so-called GFEM), created with the parametric model generation process cpacs-MONA of DLR [5]. The result of the first design loop is the baseline aircraft configuration, the GFEM is shown in Figure 3.

For a concluding assessment of the load alleviation potential, the baseline aircraft configuration has been redesigned including various load alleviation technologies, leading to the final aircraft design. The comparison of baseline and final design delivers the assessment for the potential of designing an aircraft with aggressive load alleviation [6].

3. LOAD ALLEVIATION TECHNOLOGIES

The focus of this paper is on activities in oLAF in which individual load reduction technologies have been developed, and their respective effectiveness analyzed. Promising approaches include the application of structures with non-linear properties for load reduction in wing design and the extended use of spoilers for load control. In addition, active load control laws, both feedback strategies and feedforward strategies (assuming a lidar) have been analyzed. Finally, CFD-based simulation methods to support load control have been advanced. The following sections describe the investigations in more detail.

3.1. Non-linear Stiffness in Wing Structures for Load Alleviation

With non-linear stiffnesses behaviour, the deformation of the wing structure can be influenced in such a way that a favourable lift distribution can be achieved for sizing load cases, due to a (passive) increase of the effects of bending-torsion coupling. In the project, a methodology for the introduction of materials with non-linear stiffness properties has been developed. Another approach to realize a non-linear increase of the bending-torsion coupling is the utilization of buckling to influence structural flexibility. In the post-buckling regime, the structure softens, potentially increasing the bending-torsion coupling and reducing outboard lift.

3.1.1. Non-linear Materials for Wing Structures

A method has been developed to investigate the use of materials with non-linear stiffness for aeroplane structures under load. With such an approach, the bending moment across the wing and thus the wing mass can be reduced.

With non-linear stiffnesses, the deformation of the wing structure is influenced in such a way that a favourable lift distribution is achieved for sizing load cases due to the passive mode of action. An increase in the flexibility of backward swept wings increases the effects of bending torsional coping, reducing the lift in the outer area of the wing, and in turn reducing the root bending moment.

For the mathematical derivation of the approach, the wing is currently regarded as a beam. In the approach, Hooke's law must be modified to include the non-linear elastic behaviour. The relationship between the stresses and strains is defined piecewise linear, with a series of *n* end points related to the strain for each linear sub-range, see Figure 4, [7]. Any non-linear, or better, multi-linear or piecewise linear stiffness relationship can thus be taken into account. The modulus of elasticity E can then be calculated for each linear step.

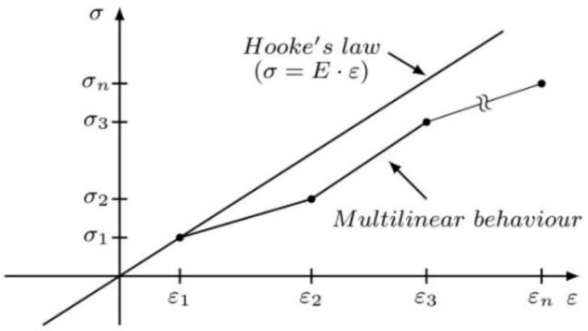

Figure 4. Hooke's law and the *n* defined regions of the piecewise linear, elastic properties

The stresses in static equilibrium must be calculated using an iterative method. The linear elastic solution is contained in the equations with *n* = 1. To allow for arbitrary bending moment distributions, the beam is analysed step by step in a finite element formulation. In the following, the approach will be called "NL Beam Method".

Figures 5 and 6 with graphs from [7] show results for an application of the approach to a medium range aircraft reference configuration. A degressive stress/strain curve is assumed for the material of the wing, i.e. one that becomes softer with increased load, see Figure 5, green curve. Figure 6 shows the resulting wing bending for the reference wing with a constant modulus of elasticity (black) compared to a wing made of a material with a softening modulus of elasticity (green).

The wings have an identical deflection for the 1 g load, maintaining aerodynamic performance. At high loads (2.5 g), though, the soft wing deflects more, which effectively shifts the load distribution inwards and thus reduces the total bending moment at the wing root due to the more pronounced washout effect. The term “washout" refers to the reduction in the local angle of attack resulting from the bending-torsional coupling of the swept-back wing.

With the approach of a degressive stress-strain relationship, a reduction of the root bending moment of 4.5 % can be achieved compared to the linear reference model. Detailed information on the method and the numerical results can be found in [7].

A corresponding material behaviour could be found in model wings made of foam materials, used to validate the mathematical approach for the description of the material properties and resulting wing deflections [8].

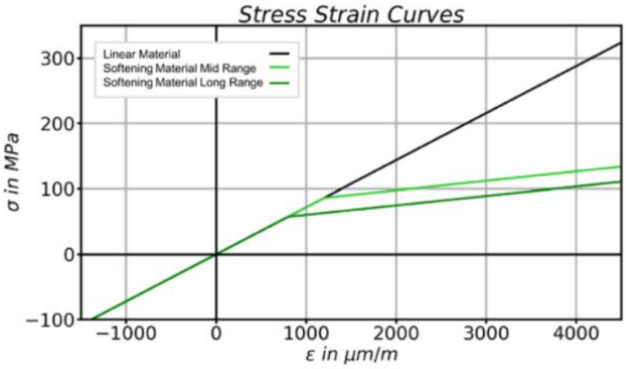

Figure 5. Application to a short and medium range aircraft configuration - stress-strain diagram

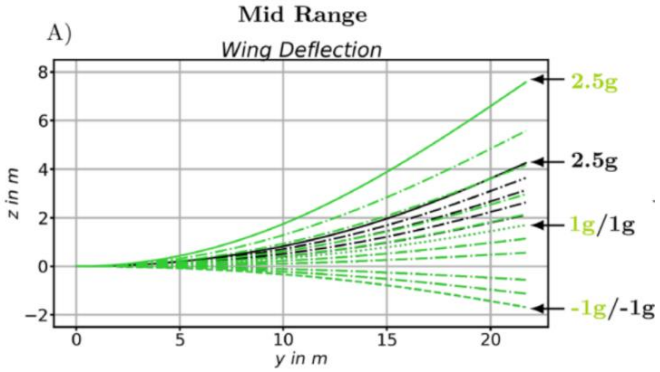

Figure 6. Resulting wing bending (black: linear material; green: non-linear material)

Due to the derivation of the method for beam structures and the current technical implementation of non-linear stiffnesses with full cross-sections made of foam materials, the technology could not be integrated into existing wing box structures with hollow cross-sections. Therefore, the technology of wings with non-linear stiffnesses has not been applied to the oLAF reference configuration described in Section 2. In principle, however, it is possible to extend the approach to other finite elements such as plate structures.

In addition, the "NL Beam Method" has also been used to describe local non-linear components. An application of the method for the description of the pressure actuators (PACS) used to operate an active folding wing tip is demonstrated in [9].

3.1.2. Structural Technologies for Higher Wing Flexibility

Another approach to realize a non-linear increase of the bending-torsion coupling is the utilization of buckling to influence structural flexibility. In the post-buckling regime, the structure softens, potentially increasing the bending-torsion coupling and reducing outboard lift. The effect is shown in Figure 7, where detailed models and non-linear buckling analyses were used. Such analyses allow the determination of stiffness reduction, but they are too computationally intensive for direct integration into structural optimization.

In order to still be able to map the effect of a buckling-critical wing structure, only a linear stiffness reduction is considered. The integration into the structural optimisation software lightworks [10] allows the evaluation of load redistribution between stringer and skin, as well as the influence on the overall stiffness.

Although the effect on the stiffness is even greater when the non-linear material laws are considered, this represents a conservative approach.

The evaluation of the potential is carried out on a representative plate of the upper shell of a current reference configuration with swept-back wings [11]. An aluminium material is used and dimensioned taking into account the Von Mises strength as well as local and global buckling criteria. The tops of the wings are stiffened with stringers. The optimized wing is shown in Figure 8 with the resulting skin thickness distribution. An optimization area with a corresponding compressive load of -371.0 kN for the 2.5 g pull-up manoeuvre was selected for the upper skin.

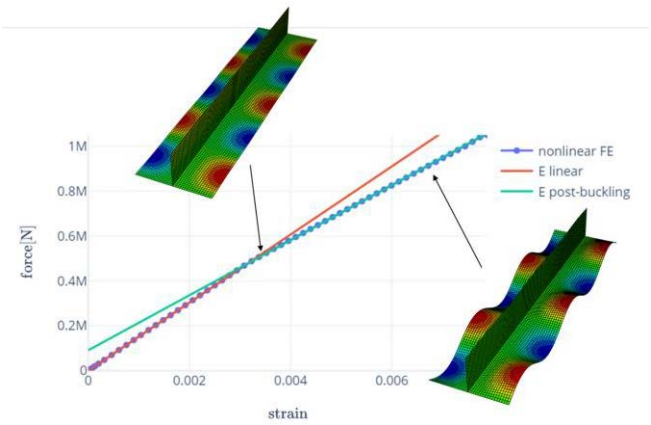

Figure 7. Non-linear buckling analysis and stiffness reduction

A stringer spacing of 0.17 m and a stiffener height of 0.05 m with isotropic aluminium material and a modulus of elasticity of 71 GPa is used. An analytical model is created based on the geometry, material properties and loads of the evaluation region. Analytical criteria such as strength and stability criteria are evaluated for all parts of the stringer. In addition, safety factors are applied to ensure the load-bearing capacity under uncertainties.

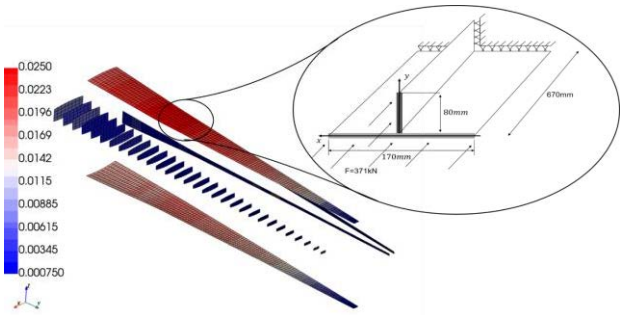

Figure 8. Example wing with thickness distribution and derived analytical panel

To analyse the mass effect of locally buckling skin panels, the safety factor of the skin is set to 1.0. This means that no buckling occurs up to limit load (actual assumed load). If the limit load is exceeded, the skin may buckle locally. However, as all strength criteria, the local buckling of the stiffening components and the global buckling are optimized against the limit load.

Table 1 shows the results of the analytical plate optimization. The reduced safety factor leads to a lower mass, as the thickness of the skin is reduced. The thickness of the stiffener is slightly increased as a load redistribution takes place due to the reduced skin thickness. The reduced safety factor ultimately leads to a mass reduction of 6.6 %.

$SF_{skin-buckling}$	parameter	value [mm]	mass [kg]
$SF = 1.5$	Thickness Skin	5.31	4.10
	Thickness Web	16.0	
$SF = 1.0$	Thickness Skin	4.49	3.83
	Thickness Web	16.0	

Table 1. Analytical results comparing different safety factors for local skin buckling

For all load cases that are not performance-relevant, the safety factor for local buckling is reduced to 0.7. This means that local buckling occurs in these load cases. The implemented sizing process works with a margin of safety (MoS), which is defined as MoS=RF-1. The reserve factor (RF) is the ratio between the critical value and the existing value, $RF=P_{critical}/P_{applied}$.

Allowing local buckling at 70 % limit load results in a required MoS of -0.3. A complete optimization, including torsion optimization, is carried out to determine the lowest fuel consumption per km and payload, which is referred to as specific fuel consumption. To reduce the numerical effort, two structural techniques are applied. An increase of the maximum allowable strain of 6100 mm/m is used for the strength analysis in combination with the reduced MoS for the local buckling of the skin. All other design criteria, such as global buckling and stiffener buckling, are kept at the level of the reference case so that they do not occur before the limit load.

Two optimizations are performed to evaluate the technologies, where the torsion distribution is optimized individually, considering the higher elasticity of the presented technologies. The optimization leads to a 2.9 % reduction in fuel consumption. The structural wing weight is reduced by 6.8 %, while the lift-to-drag ratio is improved by 0.7 %.

3.2. Investigation of Control Surfaces

3.2.1. Reduced Models for Spoilers and Bumps

Lift is conventionally reduced by the deflection of control surfaces. In addition to control surface-based technologies, bumps and microtabs are also being investigated with regard to their load reduction potential. Among other things, the focus in the process is on the provision of substitute models.

In order to quantify the benefit of the application of spoilers for load minimisation, preliminary tests were carried out on the ADIF profile [11]. Based on these findings, it was decided to further investigate the "mini flaps" technology and the "shock control bump" (SCB) technology. The mini flaps are analysed as a classic load reduction technology by calculating two correction factors for VLM from the existing steady-state results for four flap angles and four different Mach numbers for each spoiler configuration. With the help of these correction factors, spoiler deflections can now also be taken into account for load reduction in the load process with cpacs-MONA. The correction factors define the ratio in which the aeroboxes in front of and behind the spoiler should be deflected in addition to the aerobox of the spoiler.

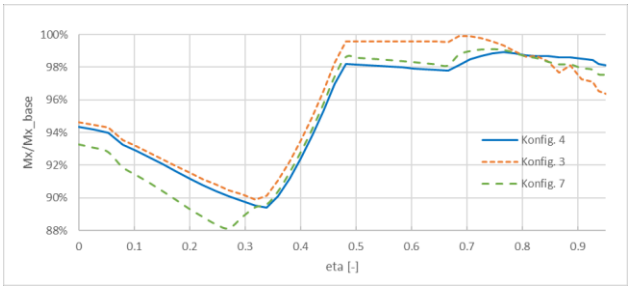

Figure 9. Envelope of the bending moment for different spoiler configurations deflected up to 30°.

By taking the flap deflections into account in the load process, it was possible to determine that the loads in the bending moment (see Figure 9) could be reduced by up to 10 %. The root bending moment is between 6 - 7 % lower, depending on the spoiler configuration (see Table 2).

Config.	*relative spoiler leading edge*	*relative spoiler chord*	*rel. spoiler trailing edge*
3	0.7	0.1	0.8
4	0.6	0.1	0.7
5	0.65	0.1	0.75
6	0.75	0.1	0.85
7	0.65	0.15	0.8

Table 2: Spoiler position and chord of investigated configurations

The application of the results in aircraft design is implemented by the use of correction factors. For this purpose, the CFD data set with all analysed spoiler configurations was transmitted to the modelling and subsequent load analysis. This serves to integrate the spoilers and their influence into cpacs-MONA. For this purpose, each data set is converted into three correction factors. The three correction factors describe the weighting of the flap deflections in the area of the spoiler, in front of and behind the spoiler, see Figure 10 (from [13]). This ensures the correct lift distribution of the Vortex-Lattice Method (VLM). In the load process, the spoilers can then also be used to reduce the load.

Figure 10. Sample visualisation for a VLM spoiler configuration with additional deflections of the aerodynamic boxes in front of and behind the spoiler

The second part of the investigations focussed on a shock control bump, see Section 3.2.2. A shock control bump was designed to reduce the wave drag. In addition, the structural concept could be designed in such a way that an even higher bump reduces lift and thus minimizes load. The results from the 2D polars were integrated in the spanwise direction to quantify the influence of the shock control bumps on a 3D wing and to compare them with the other technologies.

The lift-to-drag ratio of the aircraft was determined for different operational points, i. e. different flight altitudes (0 / 10000 / 12500 m) and flight Mach numbers (0.35 / 0.83 / 0.85). Figure 11 shows the lift-to-drag ratio of the aircraft over the lift coefficient for five different operational points. The solid lines already contain the drag of the engine nacelle and the empennage. In addition, dashed lines are drawn, which also contain and thus describe the effect of the SCB. It can be seen that for both ID3 and ID5, the bump around c_A=0.5 has a positive effect in the off-design. Here the lift-to-drag ratio increases by a few tenths. Unfortunately, no improvement can be recognised for ID2 and ID4. The improvement occurs at the higher Mach number in the off-design, at which the optimization was also carried out.

At the lower Mach number (0.83), the bump is too far forward, so that the bump in the design area does not bring any improvement.

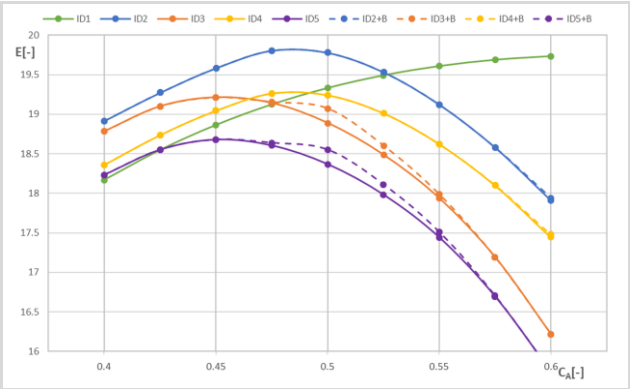

Figure 11. Lift-to-drag ratio of the four different configurations taking into account the effect of the Shock Control Bump (+B)

3.2.2. Morphing Spoiler for Drag Reduction and Load Alleviation

In order to reduce wave drag of the aircraft wing, a morphing spoiler was structurally designed which is capable of forming an adaptive shock control bump (SCB). For this purpose, a glass fibre structure with a stiffening honeycomb core was used for the stiff part of the spoiler and a pure glass fibre structure for the shape-variable, flexible part. The final configuration is shown in Figure 12, [14].

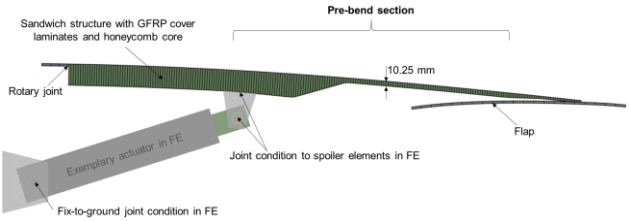

Figure 12. Finite element model of the morphing spoiler for the deployment of an adaptive shock control bump

Other configurations with a second actuator were also considered. However, it was decided that such a two-actuator concept would increase the complexity too much, so that the comparatively simple one-actuator concept was used for the final design. This concept, shown in Figure 12, has a structural pre-bend in the rear (downstream) spoiler section. This causes the trailing edge of the spoiler to stay in contact with the flap against the aerodynamic pressure loads. In addition, this pre-bend is designed to be sufficiently strong that it continues to hold the trailing edge on the flap when the actuator is deployed, thus leading to the formation of the SCB. The crest of the bump is formed just behind (downstream) the sandwich structure. The results of the finite element simulation show a very good agreement with the SCB target shape of the aerodynamicists while maintaining the structural loads within the material limitations.

In addition to the morphing designs, two reference designs were also used to evaluate the mass increase. Since conventional spoilers are not made of glass fibre but of carbon laminates, these reference spoilers were also designed using carbon. The initial approach was based on a 20%c (% of the wing profile chord) and a wing depth of 5.4202 m. However, for the final design, a spoiler only 10%c long was used and the wing chord was also set to 5.0 m. Therefore, the mass comparison in Table 3, below, shows two long (20%c) and two short (10%c) designs.

The long spoiler designs refer to a wing profile chord of 5.4202 m, while the short spoiler designs refer to a chord of 5 m. All masses are determined for a spoiler span of 2 m.

	Reference long	*Morphing long*	*Reference short*	*Morphing short*
Mass, carbon	23.3 kg	-	10.9 kg	-
Mass, glass fibre	28.1 kg	37.2 kg	13.2 kg	17.4 kg
Δ mass w.r.t. carbon reference		+13.9 kg		+6.5 kg

Table 3: Masses of spoiler designs

Table 3 shows that the long morphing spoiler is 13.9 kg heavier than the long reference. On the one hand, this is due to the higher density of the glass fibre laminate compared to carbon, and on the other hand, a comparatively thick laminate is required downstream the sandwich structure (see Figure 12) in order to be able to bear the loads during the air brake. With the short designs, the morphing spoiler becomes 6.5 kg heavier. If the latter is assumed for a total of six spoilers (three per wing), this results in a total weight increase of +39 kg. In order to consider possible additional masses for components neglected in this analysis, such as sensors or cables, a mass increase of +50 kg was assumed for the entire aircraft.

In the aircraft design task, the potential of adaptive SCBs on morphing spoilers was estimated. For this purpose, the +50 kg weight increase resulting from the structural design due to the morphing system (on a total of six spoilers) was taken into account. In addition, drag data was transferred to the aircraft design task. This did not result in any significant improvements in terms of drag reduction and the associated fuel and consequently weight savings in the design area of the aircraft. However, a certain potential for the off-design area could be determined.

3.3. Active Load Control

Two groups of active load control algorithms are investigated in oLAF, first feed-back control laws, working on the basis of immediate feed-back of measured data, e.g. accelerometers on the wing, second feedforward control algorithms making use of data acquired before an excitation hits the aircraft and the wing.

3.3.1. Robust Gust Load Reduction Through Feedback Control

This section focusses on the robust, automated design of a Gust Load Alleviation (GLA) feedback controller suitable for the MDO chain and presents the results of the load analysis with and without the GLA controller. For the development of load alleviation systems, two goals are addressed: First, a reduction of structural loads, which enables a lighter design of aircraft wings. Second, reduced loads can improve passenger comfort.

The controller design is based on a linearized, aeroelastic aircraft model in state-space form. The state-space model is derived using a finite element model for the structure and a vortex lattice / double lattice (VLM / DLM) model for the aerodynamics. Thus, the aerodynamic forces are originally defined in the frequency domain and have been transferred to the time domain by rational function approximation for the aircraft part and a Loewner approximation for the representation of the gust.

Such a linear model is generally much easier to analyse, control and simulate than a non-linear model. Different mass configurations at different predefined flight points, i. e. combinations of cruise altitudes and airspeeds, serve as input for the design of parametric load reduction controllers. The model is then augmented into a so-called aeroservoelastic aircraft model by the introduction of sensor and actuator dynamics.

The main objective of the load control design activities is to minimise the structural loads resulting from gust excitations, i. e. to minimise the occurring wing root bending moment during a vertical 1-cos gust passage according to EASA CS-25 [15]. Secondary objectives include the damping of the overall structural response, minimising the torsional moment in the wing root and improving passenger comfort, e.g. minimizing the overall aircraft reaction such as the centre of gravity acceleration due to the vertical wind excitation.

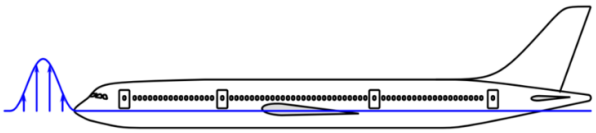

Figure 13. Schematic representation of a vertical (1-cos) gust entry

The feedback controller synthesised for this is a state-space model with a gain matrix, analogous to a P-controller, which requires the vertical load multiple n_z (load factor) as input. Aileron and elevator deflections, see Figure 14, are calculated as outputs. The linearized actuator dynamics as well as the limiting maximum control surface deflections and control surface rates were also taken into account. In order to cover the entire flight envelope, the gust load calculations are carried out and analysed with different mass configurations m_{config} (here: 6 mass cases) and at predefined flight altitudes h (here: $n_{altitude}$=5) with three flight speeds v_B, v_C and v_D in each case. In the a priori performed gust simulation campaign according to EASA CS-25, six gust gradients H were considered at each flight point. For the controller design, initially only vertical (upwards and downwards) 1-cos gusts were considered. This results in a total of 1080 gust load cases, from which the critical load cases are determined. For the critical load cases, linearized state-space models are then generated, see above, which are used for the controller synthesis. Various optimization methods were implemented based on the framework of linear matrix inequalities (LMIs) and the loop shaping procedure of McFarlane and Glover [16]. All methods have been implemented in Matlab. Depending on the method, the Ro-

bust Control Toolbox from Matlab, the freely available LMI Toolbox YALMIP and the Mosek Solver, the Model Order Reduction Toolbox from ONERA, or the Multi-Objective Parameter Synthesis (MOPS) optimization software from DLR are required.

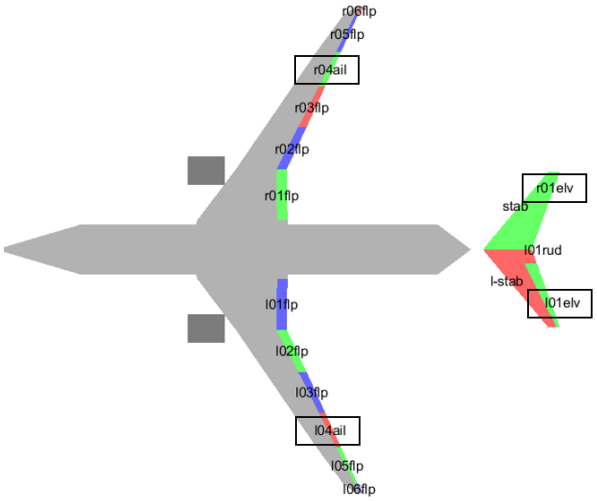

Figure 14. Control surface configuration of the oLAF reference model for the MDO chain (only the control surfaces highlighted by boxes are used by the GLA controllers)

Figure 15 below visualises the maximum bending moments for the critical load cases with (CLP = closed-loop) and without (OLP = open-loop) the feedback GLA controller for the (right-hand) wing of the baseline design of the oLAF reference model. The bending moment at the wing root could be reduced by 18.8 % to 25.3 % with the help of the feedback GLA controller. As already described at the beginning, these results only apply to the eight critical cases that are driving the maximum wing root bending moment.

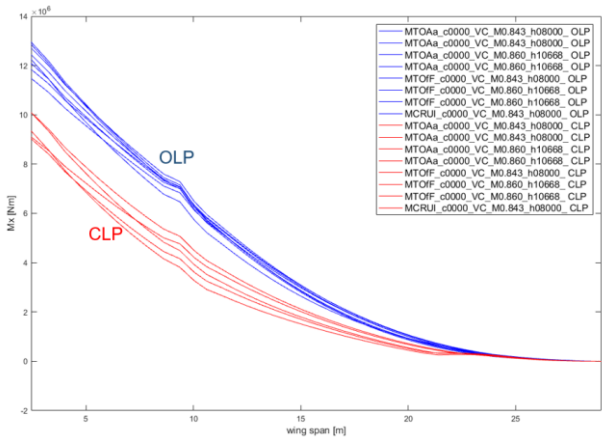

Figure 15. Bending moment curve with and without feedback GLA controller for the critical load cases on the right wing

In the oLAF project, the active load alleviation methods could not be directly applied for the structural sizing of the reference aircraft design task, described in Section 2, above. However, although no actively controlled loads were used in the aircraft design, a comparable level of load reduction was achieved by means of a similar, quasi-static approach. The active load reduction methods were made available for the MDO developments, see Section 5. Most notably, the design procedures for the load controllers were validated in the NWB wind tunnel test, see Section 4, in which a substantial load reduction could be demonstrated by feedback control.

3.3.2. Doppler Wind Lidar with Wind Estimation Algorithm

The technology of the Doppler wind lidar with wind estimation algorithm is the prerequisite for all GLA methods based on preview control. From the relative speeds of the wind field measured with the lidar sensor in relation to the aircraft (or the sensor), a vertical wind profile is created using a wind reconstruction algorithm [17], which is made available to the feedforward GLA controller as an input signal before the gust encounter. The anticipation time thus available can be used to realise a partial pre-compensation of the expected gust-induced angle of attack variation (lift force variation, utilizing mainly the elevator). The wings experience an overall reduced structural peak load distribution during the gust passage.

An integrated GLA simulation environment was created in MATLAB/Simulink, which includes an arbitrary aeroelastic aircraft model, GLA controller(s), actuators, as well as the lidar sensor with wind reconstruction algorithm, which can be used to evaluate the performance of the GLA system. The lidar model and the wind reconstruction algorithm are implemented in C++, the interfaces to the Simulink environment work via a Simulink S function (also C++). This simulation environment was later fully implemented in C++ as part of the MDO task, see Section 5, in order to improve computational performance and to enable operation on the CARA high-performance computer system [18] without having to rely on MATLAB/Simulink licences. The resulting tool was named A²LARMS (Assessment of Active Load Alleviation through Multi-rate Simulation).

The lidar sensor model was developed in collaboration with the DLR Institute of Atmospheric Physics as part of the COLOCAT project. It is a simplified (but nevertheless realistic) surrogate model that was developed on the basis of a very complex simulation of the lidar ("end-to-end simulator") [19]. This end-to-end simulator maps almost the entire measurement process on a physical level on the basis of Monte Carlo simulations and is unsuitable for use in the above-mentioned integrated GLA simulation environment due to the associated high computational effort. Therefore, for A²LARMS (and such evaluations in general), the aforementioned substitute model is used, which provides a realistic representation of the lidar with low computational effort [20].

The investigations into the optimum parameter range of the lidar and the wind estimation algorithm for use in oLAF were well supported by the knowledge already gained in COLOCAT, so that an optimized set of parameters could be identified. For this purpose, an evaluation metric was first developed [21] and then sensitivity studies were carried out. Some of the results of the sensitivity studies were presented at IFASD 2022 [22].

When designing the feedforward controller, knowledge about the behaviour of the feedback controller (Section 3.3.1) operating in parallel was considered in order to implement a pre-compensation that ensures that the two controllers do not work against each other during opera-

tion [23]. Knowledge of the transfer function of the lidar system was also used in the controller design in order to optimally utilise the potential of the sensor [24].

To evaluate the load reduction potential, the aircraft configurations from both tasks were evaluated with the integrated simulation environment A²LARMS. For this purpose, a separate feedforward controller was designed for each of the two configurations, which works together with the feedback controllers also specially designed for this purpose. When designing the feedforward controllers (as well as the integration with the feedback controllers), attention was paid to good-natured behaviour, i.e. aggressive control commands were avoided. In addition, the feedforward controller only reacts to disturbances (e.g. turbulence) above a certain threshold value in order to avoid unnecessary actuator movements and the associated wear.

The overall potential was evaluated by simulating gust passages for those load conditions and flight points that previously showed the most critical loads. Here, a 16.3 % reduction in the root bending moment was achieved for the final design of the reference configuration (see Section 2) and as much as 20.0 % for the MDO configuration. Selected results are shown in Figure 16 for the MDO configuration (see Section 5), using the combined feedforward/feedback controller.

It can be assumed that even greater load reduction potential could be achieved with more aggressive tuning, but this is deliberately not done, as the relatively small gain in load reduction would not outweigh the inevitably higher actuator wear associated with it.

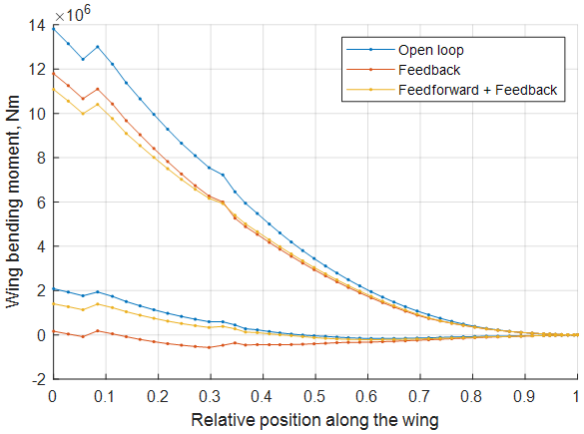

Figure 16. Envelope of the bending moment (right wing), MDO configuration

To date, there are no series-produced lidar-based load reduction systems. However, there is great interest from the industry, which is why more work has been done in recent years to mature the technology. In the Clean Aviation project UPWing (Ultra Performance Wing), in which the lidar and load reduction topics are of great importance, work is being carried out on increasing the TRLs of these technologies in order to enable their use in the next generation of commercial aircraft.

3.4. Numerical Approaches for Analysis of Load Alleviation

The technology development described so far is supported by improvements in CFD-based simulation approaches. Active load control devices operate by introducing a local influence on the flow field which can only be analysed with sufficient quality using CFD analyses. This is especially true in the transonic regime. The aim of the work on oLAF is to create suitable CFD-based unsteady aerodynamic models that can be used with parametric structural models to evaluate the various load control approaches.

3.4.1. CFD-based Reduced Models for Classical Control Surfaces

A surrogate model is developed to calculate and determine the static and dynamic response behaviour for any flight conditions of moving geometries, such as flap deflection or the pitching motion of an aircraft, and set up pre-calculated databases. The data generation is performed using the Linear Frequency Domain Solver (LFD) developed at DLR [25] to achieve a high level of accuracy for dynamic response, based on a RANS calculation. In this way, aerodynamic coefficients and surface pressure distributions for any control surface deflections can be efficiently calculated and reused. From the databases, a calculation of those data is performed within milliseconds and therefore enables a wide range of applications, whether for optimization or in real-time experiments. The process is depicted in Figure 17 and described in [26]. The LFD surrogate model technology is used intensively for the oLAF wind tunnel test concentrating on control surface transfer functions and for the highly dynamic FlapTab.

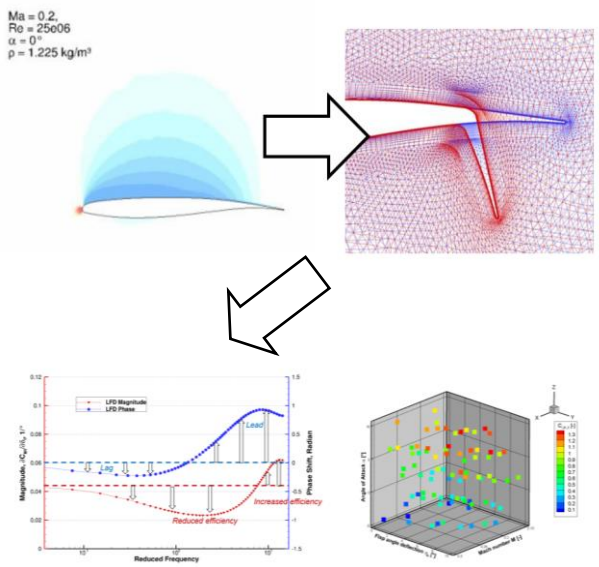

Figure 17. Generation of the database: RANS-Solution → definition of motion → calculation of ĝ-vector with LFD → include data point

The theory and technology of the surrogate model was developed, extensively tested and analysed in the internal project Load Adaptive Wing. The principles and functionalities of the surrogate model were presented in a journal article for the control surface surrogate model [26]. The

model was extended by the prediction of the gust response and a combined gust load reduction by control surface deflection, which was presented in another publication [27].

The LFD surrogate model was used extensively for the wind tunnel test of the highly dynamic FlapTab in this project. The tests were conducted in a low-speed wind tunnel and investigated the unsteady aerodynamic responses for dynamic control surface deflections.

During the investigation, a number of conclusions could be drawn about the dynamic behaviour of control surfaces for load reduction:

Higher control surface rates must be reached before the first dynamic effects occur in the aerodynamics. At higher speeds, the control surface first loses effectiveness in generating lift, until at a certain rate, the effectiveness increases again and becomes increasingly higher. Similarly, as the deflection rates increases, the response of the lift generation initially runs behind the flap movement in terms of time until it then has no phase shift again and even runs in phase "ahead" of the input signal. The absolute time delay of the response decreases with increasing oscillation frequency.

An increase in the control surface area leads to an increase in effectiveness, but less than proportional to the increase in size. In most applications, the dynamic effects only have a minor influence on the pitching moment generation (on the wing) due to fast control surface deflections.

If a shock occurs at higher Mach numbers, the effectiveness of the control surface is significantly reduced. When the spoiler is deflected by 30°, the effectiveness of the flap for generating lift is also reduced by more than half, as the upper side of the control surface is in the flow separated area.

A real 3-dimensional control surface is less effective at generating lift than the same geometry in a real 2D section. The effectiveness approaches the value of the 2D section when the real control surface becomes larger across the span.

The surrogate model is provided to the other work packages as a usable technology. If necessary, a new surrogate model can be set up and made available for the respective case. The surrogate models are analysed and used in detail to support and compare them with the wind tunnel experiments. The wind tunnel experiments work with fast-moving control surfaces and possible gusts and can therefore be modelled very well with the surrogate model and calculated efficiently. In the MDO task, a possible application of the surrogate model in preliminary design tools for determining the effectiveness of load reduction is planned, as the aerodynamic reaction of the wing to gusts and control surface inputs can be substituted here with the same speed but with greater accuracy compared to manual methods.

3.4.2. CFD-based Fast Models to be Used for Active Load Reduction and Flutter Control

Composite materials make it possible to change the elastic material properties in the structures. This opens up the possibility of passively improving the coupled aerostructural properties (e. g. aeroelastic tailoring). In addition, active control can be used to alleviate loads. In order to evaluate the potential of passive and active technologies for aircraft flying in the transonic range, CFD-based modelling must be used. The aim of the work described in the following is to create suitable CFD-based unsteady aerodynamic models that can be used with parametric structural models for the design and evaluation of control technologies. Furthermore, a wing designed with aggressive load alleviation must still be free from flutter. Thus, methods are developed at DLR to calculate the flutter boundary with a novel, CFD-based fast method, and to determine the flutter sensitivities for a 3D wing model.

The recently developed techniques for generating reduced-order aeroservoelastic models can easily be used with high accuracy aerodynamic CFD data, which is mandatory in the transonic domain. In particular, the linear frequency domain solver (LFD) generates the required data in the frequency domain. The focus here is on the methodology that enables the design of a controller with an aeroservoelastic model in which highly accurate unsteady LFD aerodynamics are embedded.

The reduced-order model contains the aerodynamic data and thus enables analytical coupling with a range of parametric structural models, allowing the potential load reduction achieved with different designs and with existing control laws for active load reduction to be determined. The method for creating reduced order aeroelastic models in state-space form is described in [28].

The application of the techniques based on the Loewner framework was applied to a gust input and, as expected, showed an excellent agreement of the reduced-order state-space model with the LFD reference data, although the complex LFD data show the spiral behaviour caused by the gust penetration effect. This is due to the fact that the proposed method does not require the user to select the aerodynamic lag poles, but instead generates them automatically from the tangential interpolation conditions.

Figure 18 shows complex data from the reduced-order model in aeroelastic state-space formulation (Loewner) compared to the reference data in the frequency domain (FD) for the transport aircraft configuration CRM/FERMAT flying at a transonic Mach number of Ma = 0.86 with an angle of attack of 1.641°, at an altitude of 9100 m and showing a strong shock. The gust length is given by H=350 ft and for an equivalent amplitude of 1°.

The resulting aeroservoelastic model (including transfer functions for sensors and actuators) was used to perform an H_∞ framework for controller synthesis to reduce gust loads in a vertical gust encounter. In particular, the controller synthesis already includes the transient transonic aerodynamics of the LFD.

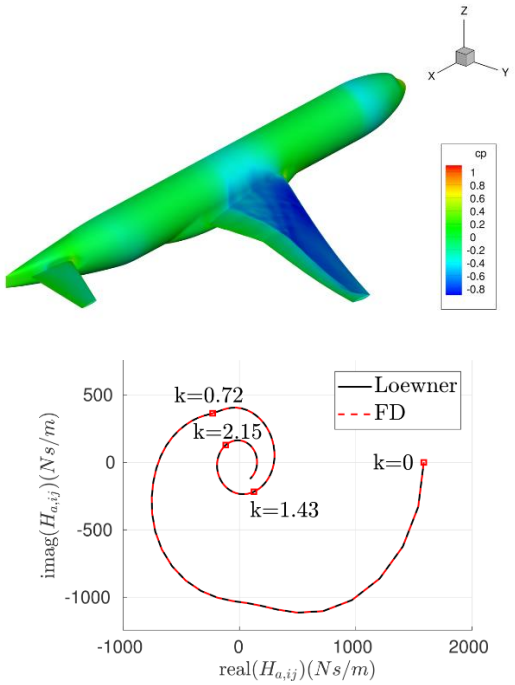

Figure 18. Complex data from the reduced-order model in aeroelastic state-space formulation

Figure 19 and Figure 20 show the reduction of the so-called generalized aerodynamic forces (GAF), i. e. the physical forces projected onto the first flexible component achieved by a static controller with power feedback. The considered (1-cos) gust has an amplitude of 10 m/s and a main frequency of 2 Hz. The highest peak is reduced by 8 % with the current controller. Further reductions can be expected by using other sensors and taking dynamic conditions into account in the controller.

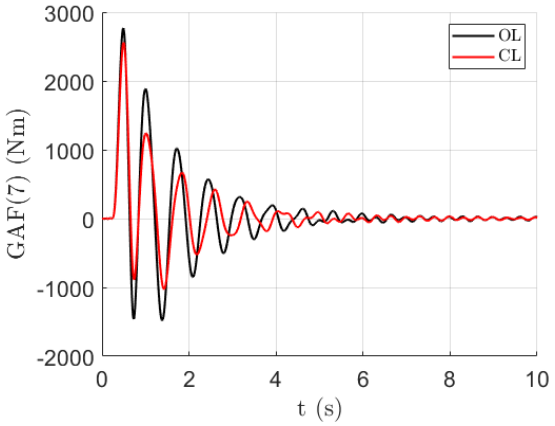

Figure 19. Open-loop (OL) and closed-loop (CL) simulations showing the reduction of the GAF component projected onto the first flexible mode

Furthermore, a new methodology for the CFD-supported flutter analysis was developed. The so-called *p-L* method [29] was applied to this configuration for flutter analysis, demonstrating its effectiveness when used with transonic aerodynamics obtained via LFD. The flutter sensitivities related to the *p-L* method have been presented in [30], though they have not been integrated into the MDO process. Additionally, as recently shown in [31], this flutter solution method allows for the simultaneous computation of both flutter and buffet onset values.

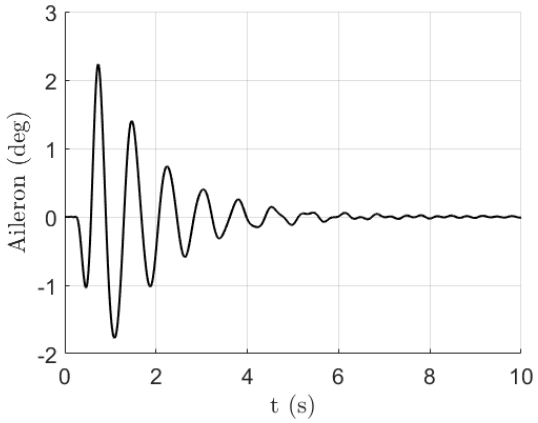

Figure 20. Aileron deflection commanded by the controller to reduce gust loads

Finally, a procedure has been developed to precisely determine the flutter sensitivities with regard to parameters in the aircraft design. In the project, a dependence of the flutter speed on wing planform parameters was developed for the MDO task, see Section 5. In this context, the flutter sensitivities were determined using the p-k method, based on DLM models. The results of the analyses of 2D and 3D configurations as well as the planform parameters were published [32].

4. WIND TUNNEL EXPERIMENTS

The design of efficient load control approaches requires detailed knowledge about the involved physical effects. For the current investigations, the focus of the experimental, i. e. wind tunnel, activities was on the identification of unsteady control surface aerodynamics and the validation of respective CFD analyses, and on the validation of control design algorithms suggested for use in load control on a full aircraft scale. An overview of the activities is given in [33].

Control surface transfer functions

For the evaluation of the effectiveness of control surface based measures for load reduction and adequate controller design, precise and well-founded knowledge of the transfer behaviour of the corresponding control surfaces across all flight ranges is of decisive importance. Measurement data from past fundamental experiments in the DNW-NWB (e.g. subsonic for spoilers) and the transonic wind tunnel DNW-TWG (e. g. transonic for dynamic control surface oscillations) already exist for individual devices and ranges of application and have been evaluated in the first phase of the oLAF project.

First, available data for dynamic control surface motion in transonic speed was evaluated. The data originates from the so-called COSDYNA (COntrol Surface DYNAmics) experiments, a series of experiments conducted in collaboration with the former Département Aéroélasticité et Dynamique des Structures (DADS) of ONERA, France, and with JAXA, Japan. The aim was to create a high-value experimental database for motion-induced forces on trailing-edge control surfaces in transonic flow. The data is intended for the validation of numerical simulation meth-

ods and as a reference data set for flutter and load prediction for aircraft structures and control surfaces [34].

Second, a dedicated wind tunnel campaign was performed for the identification of unsteady spoiler aerodynamics, validating the numerical simulations described in Section 3 above. To expand the experimental database in the low-speed range, the aerodynamic response behaviour is measured during dynamic deflections of control surfaces (optionally with a deflected spoiler). For this purpose, the trailing edge flap of the 2D airfoil model of the DLR-F15 with a span of 2.8 m and an airfoil chord of 0.6 m has been fitted with a camber tab. With this model setup, the dynamic response behaviour of the flow is measured and analyzed in detail at speeds of up to 90 m/s in the DNW-NWB. The data obtained allow the calculation methodology and the dynamics of the control surfaces predicted in to be validated.

Demonstration of active load alleviation functions

In a second wind tunnel experiment the effectiveness of different active control approaches with regard to the reduction of structural loads has been evaluated. The aim of the experiment was to demonstrate that a wing designed for load reduction, with the dynamic properties of the control surfaces determined numerically and applying the corresponding controller synthesis methodologies, is capable of reducing gust and manoeuvre loads as predicted.

The basis for the wing design is the long-range reference aircraft described in Section 2. The planform of the wind tunnel wing is derived from the overall aircraft design, see Figure 2, scaled to wind tunnel dimension. However, the implementation of the active components requires a certain model size, thus the demonstrator test is carried out with a half-model configuration. The choice of a half model is also favourable in another context as it allows a more flexible wing to be designed for the given strength requirements.

The experiment was performed in the subsonic DNW-NWB wind tunnel. The preparation of the experiment, the development of a gust generator for the wind tunnel, the development of the control algorithms and selected test results have been presented in a series of publications at the IFASD 2024 [35] - [38].

5. LOAD ALLEVIATION IN THE MULTI-DISCIPLINARY WING DESIGN AND OPTIMIZATION PROCESS

Multidisciplinary design optimization (MDO) has been much advanced in the past years. In oLAF, the existing cross-institute multidisciplinary aircraft design tools are improved by adding new technologies and applying them to a new configuration. Furthermore, the tools' capabilities towards dealing with load alleviation during the automatic multidisciplinary wing design process are extended. DLR's cross-institute gradient-based multidisciplinary design optimization (MDO) chain is presented in Figure 21. The process involves mainly two parts; the first ensures the structure integrity and the second predicts and improves the flight performance, mainly at cruise and off-design points. The structure integrity is handled via the "Structure Loads & Sizing" and "Flutter Analysis" components shown in Figure 21. The flight performance is predicted here via coupling a RANS-based flow solver (DLR's TAU code) with the structure solver NASTRAN in order to account for the elastic deformations of the aircraft in flight, and with the 1D thermodynamic engine model, to exchange thrust and engine boundary conditions while trimming the aircraft forces. The shape improvement is predicted based on the design sensitivities, which require a differentiation of the numerical models engaged.

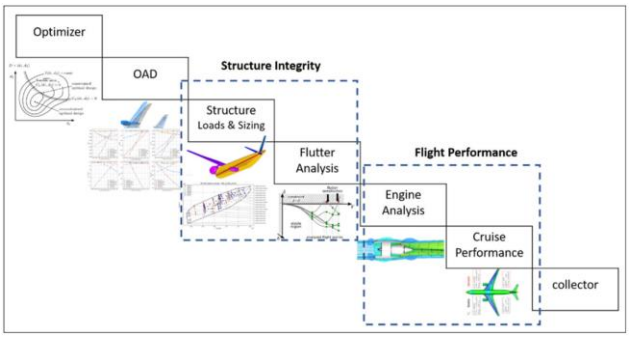

Figure 21. Block diagram of the cross-institute gradient-based MDO chain

On the structure integrity side, two main aspects are pursued. The first one is to model the structure via composite materials, either while dealing with it as a smeared thickness or while giving the designer more freedom to tackle the different layers nearly independently. The second aspect is to enhance the loads prediction process with load alleviation tools that allow the designer to investigate the feasibility of such systems in a robust and automatic design process. On the flight performance side, the focus lies on enhancing the aircraft trim process, while engaging the sizing of the engine and all the modelling complexities related to that, in the design loop.

An overview of the capabilities of DLR's cross-institute multidisciplinary design optimization chain at the beginning of the oLAF project is given in [39]. A summary of the developments and results achieved during the oLAF project is presented in [40].

6. CONCLUSION

In the project oLAF, specific technologies for load reduction have been developed and made available to the other work packages of the project, i.e. aircraft design, wind tunnel tests, and MDO processes.

Passive load alleviation techniques are promising, and while aeroelastic tailoring using linear materials is state-of-the-art, taking advantage of non-linear materials or structural phenomena like buckling is still a topic of research, albeit a promising one. The use of dedicated control devices like multi-functional spoilers is a realistic development. If the benefit can be shown, a near-term application is realistic. Concerning control, active load control will be an integral part of future wing development. While feedback control already leads to considerable load reduction, the application of lidar technology and the corresponding feed forward control will be a game changer towards lower gust loads and thus lighter structures. The extensive use of CFD, both for fast methods (surrogate models) and for control design (state-space-models) will be an indispensable support in design as transonic phenomena are captured which strongly influence load analysis and control.

7. REFERENCES

[1] Schulze, M., Klimmek, T., Torrigiani, F., Wunderlich, T.F. (2021): Aeroelastic Design of the oLAF Reference Aircraft Configuration. Deutsche Luft- und Raumfahrtkongress, DLRK 2021, Bremen, Germany. https://elib.dlr.de/143642/

[2] Wunderlich, T. (2022): Multidisciplinary Optimization of Flexible Wings with Manoeuvre Load Reduction for Highly Efficient Long-Haul Airliners. Deutscher Luft- und Raumfahrtkongress 2022, Dresden. https://doi.org/10.25967/570055

[3] Schulze, M., Handojo, V. (2023): Aeroelastic Design of the oLAF Configuration using Load Alleviation Techniques within cpacs-MONA. Presentation at the Deutsche Luft- und Raumfahrtkongress, DLRK 2023, Stuttgart, Germany. https://elib.dlr.de/198111

[4] Alder, M., Moerland, E., Jepsen, J., Nagel, B. (2020): Recent Advances in Establishing a Common Language for Aircraft Design with CPACS. Aerospace Europe Conference, 25-28.02.2020, Bordeaux, Frankreich. https://elib.dlr.de/134341/

[5] Klimmek, T., Schulze, M., Abu-Zurayk, M., Ilic, C., Merle, A. (2019): cpacs-MONA – An independent and in high fidelity based MDO tasks integrated process for the structural and aeroelastic design for aircraft configurations. International Forum on Aeroelasticity and Structural Dynamics, IFASD 2019, Savannah, GA, USA. https://elib.dlr.de/128099/

[6] Himisch, J. (2024): Zum Potential der Berücksichtigung von Lastabminderungstechnologien im Flugzeugentwurf: Performancesteigerungsuntersuchungen am Beispiel einer Langstreckenkonfiguration. Deutscher Luft- und Raumfahrtkongress, DLRK 2024, 30.9.-2.10.2024, Hamburg.

[7] Bramsiepe, K., Klimmek, T., Krüger, W.R., Tichy, L. (2022): Aeroelastic Method to Investigate Nonlinear Elastic Wing Structures. CEAS Aeronautical Journal. 2022. Springer. https://doi.org/10.1007/s13272-022-00596-0

[8] Bramsiepe, K., Braune, M., Krüger, W.R., Tichy, L. (2022): Wind tunnel experiment with an EPP-wing to investigate aeroelastic effects of nonlinear elastic stiffnesses. In: 33rd Congress of the International Council of the Aeronautical Sciences, ICAS 2022. ICAS 2022, 2022-09-04 - 2022-09-09, Stockholm, Schweden. https://elib.dlr.de/189396/

[9] Meyer, P., Hühne, C., Bramsiepe, K., Krüger, W.R. (2023): Aeroelastic Analysis of Actuated Adaptive Wingtips Based on Pressure Actuation. Journal of Aircraft. American Institute of Aeronautics and Astronautics (AIAA). https://doi.org/10.2514/1.C037390

[10] Dähne, S., Werthen, E., Zerbst, D. et al. (2024): Lightworks, a scientific research framework for the design of stiffened composite-panel structures using gradient-based optimization. Struct Multidisc Optim 67, 70 (2024). https://doi.org/10.1007/s00158-024-03783-1

[11] Bramsiepe, K., Gröhlich, M., Dähne, S., Hahn, D. (2022): Structural Concepts for Passive Load Alleviation. AIAA SCITECH 2022 Forum, 3.-7. Jan. 2022, San Diego, CA & Virtual. https://doi.org/10.2514/6.2022-0687

[12] Richter, K. und Rosemann, H. (1999): Widerstandsreduzierung an einem transsonischen Profil durch die kombinierte Anwendung von variabler Wölbung und Konturbeule. 9. STAB-Workshop, 9.-11.10.1999, Göttingen.

[13] Schulze, M., Handojo, V., Goerttler A. (2024): CFD-Based Spoiler Corrections for Load Alleviation within cpacs-MONA, Deutscher Luft- und Raumfahrtkongress, DLRK 2024, 30.9.-2.10.2024, Hamburg.

[14] Künnecke, S.C., Schäfer, M., Goerttler, A., Waldmann, A., Vasista, S., Riemenschneider, J. (2023): Concept of a Morphing Shock Control Bump Spoiler with Two Actuators. 10th ECCOMAS Thematic Conference on Smart Structures and Materials, SMART 2023, 3-5 July 2023, Patras, Greece. https://elib.dlr.de/196950/

[15] Easy Access Rules for Large Aeroplanes (CS-25). Published November 2018, updated on 30 January 2023. https://www.easa.europa.eu/en/downloads/66796/en

[16] Glover, K., McFarlane, D. (1989): Robust Stabilisation of Normalized Coprime Factor Plant Descriptions with H∞-Bounded Uncertainty. IEEE Trans. Autom. Contr., Vol. 34, 1989.

[17] Fezans, Nicolas und Joos, Hans-Dieter und Deiler, Christoph (2019) *Gust load alleviation for a long-range aircraft with and without anticipation.* CEAS Aeronautical Journal. Springer. https://doi.org/10.1007/s13272-019-00362-9

[18] https://www.dlr.de/en/research-and-transfer/research-infrastructure/hpc-cluster/cara

[19] Cavaliere, Davide und Fezans, Nicolas und Kiehn, Daniel und Quero-Martin, David und Vrancken, Patrick (2022) *Gust Load Control Design Challenge Including Lidar Wind Measurements and Based on the Common Research Model.* AIAA SciTech, 03.-07.01.2022, San Diego, California, USA. https://doi.org/10.2514/6.2022-1934

[20] Wallace, C., Schulz, S., Fezans, N., Kier, T., Weber, G. (2022): Evaluation Environment for Cascaded and Partly Decentralized Multi-Rate Load Alleviation Controllers. 33rd Congress of the International Council of the Aeronautical Sciences (ICAS), 04.-09.2022, Stockholm, Schweden. https://elib.dlr.de/188264/

[21] Kiehn, D., Fezans, N., Vrancken, P. (2012): Frequency-domain performance characterization of lidar-based gust detection systems for load alleviation. Deutscher Luft- und Raumfahrtkongress (DLRK), 31.08.-02.09.2021, Bremen/virtuell. https://elib.dlr.de/148352/

[22] Kiehn, D., Fezans, N., Vrancken, P., Deiler, C., (2022): Parameter Analysis of a Doppler Lidar Sensor for Gust Detection and Load Alleviation. In: 19th International Forum on Aeroelasticity and Structural Dynamics (IFASD), 13.-17.06.2022, Madrid. ISBN 978-840942353-8. https://elib.dlr.de/187627/

[23] Wallace, C., Fezans, N. (2024): Lidar-Based Gust Load Alleviation - Increasing the Load Reduction Potential through a Two-Degree-of-Freedom Controller Architecture. 20th International Forum on Aeroelasticity and Structural Dynamics (IFASD 2024), 17.-21.06.2024, The Hague, The Netherlands.

[24] Cavaliere, D., Fezans, N., Kiehn, D. (2022): Method to Account for Estimator-Induced Previewed Information Losses - Application to Synthesis of Lidar-Based Gust Load Alleviation Functions. In: 6th CEAS Conference on Guidance, Navigation and Control (EuroGNC), 03.-05.05.2022, Berlin.
https://elib.dlr.de/193034/

[25] Widhalm, M., Bekemeyer, P., Seidler, R.B., Marten, S. (2020): Linear Frequency Domain Method For Aerodynamic Applications. WCCM & ECCOMAS 2020, 11.-15.01.2021, Paris.

[26] Seidler, R.B., Marten, S., Widhalm, M., Wild, J. (2020): Efficient Prediction of Aerodynamic Control Surface Responses Using the Linear Frequency Domain. AIAA Journal, 58 (5). American Institute of Aeronautics and Astronautics (AIAA).
https://doi.org/10.2514/1.J058840

[27] Seidler, R.B., Widhalm, M., Wild, J. (2020): Load Control for Unsteady Gusts with Control Surfaces using the Linear Frequency Domain. In: AIAA Aviation 2020 Forum. AIAA Aviation 2020 Forum, 15.-19. Juni 2020, Virtual Event.
https://doi.org/10.2514/6.2020-2670

[28] Quero, D., Vuillemin, P., Poussot-Vassal, C. (2019): A generalized state-space aeroservoelastic model based on tangential interpolation. Aerospace 6, 1.
https://doi.org/10.3390/aerospace6010009

[29] Quero-Martin, D., Vuillemin, P., Poussot-Vassal, C. (2021): A generalized eigenvalue solution to the flutter stability problem with true damping: The p-L method. Journal of Fluids and Structures, 103 (103266). Elsevier.
https://doi.org/10.1016/j.jfluidstructs.2021.103266

[30] Quero, D., Vuillemin, P., Poussot-Vassal, C. (2022): Improved mode tracking for the p-L flutter solution method based on aeroelastic derivatives. In: 19th International Forum on Aeroelasticity and Structural Dynamics, IFASD 2022. International Forum on Aeroelasticity and Structural Dynamics (IFASD) 2022, 13.-17.06.2022, Madrid, Spain.
https://elib.dlr.de/187885

[31] Quero, D., Kaiser, C., Nitzsche, J. (2024): A general solver for the prediction of flutter and buffet onset. 20th International Forum on Aeroelasticity and Structural Dynamics (IFASD 2024), 17.-21.06.2024, The Hague, The Netherlands.
https://elib.dlr.de/205025

[32] Kaiser, C., Quero, D. (2022): Effect of Aerodynamic Damping Approximations on Aeroelastic Eigensensitivities. Aerospace 2022, 9, 127.
https://doi.org/10.3390/aerospace9030127

[33] Mai, H., Altkuckatz, A., Braune, M., Dillinger, J., Friedewald, D., Hanke, C., Kirmse, T., Klein, C., Krüger, W.R., Michel, K., Micheli, B., Ritter, M., Schmalz, M., Schmidt, T.G., Seidler, R.B., Stalla, F.J., Waitz, S. (2024): Bewertung der Wirksamkeit von steuerflächenbasierten Maßnahmen zur Lastabminderung. Deutscher Luft- und Raumfahrtkongress, DLRK 2024, 30.9.-2.10.2024, Hamburg.

[34] Altkuckatz, A., Braune, M., Mai, H. (2022): Management, archiving and provision of aerodynamic and aeroelastic data - A new database concept. 19th International Forum on Aeroelasticity and Structural Dynamics, IFASD 2022. International Forum on Aeroelasticity and Structural Dynamics, IFASD 2022, Madrid, Spain.
https://elib.dlr.de/187733/

[35] Krüger, W.R., Mai, H., Kier, T., Reimer, L. (2024): Assessment of Active Load Control Approaches for Transport Aircraft – Simulation and Wind Tunnel Test. International Forum on Aeroelasticity and Structural Dynamics, IFASD 2024, Den Haag, The Netherlands.
https://elib.dlr.de/206124/

[36] Dillinger, J., Mai, H., Krüger, W. R., Schmidt, T. G., Stalla, F. (2024): Design, manufacturing and identification of an actively controlled flexible wing for subsonic wind tunnel testing. International Forum on Aeroelasticity and Structural Dynamics, IFASD 2024, Den Haag, The Netherlands.
https://elib.dlr.de/205840/

[37] Schmidt, T.G., Dillinger, J., Ritter, M., Altkuckatz, A., Hanke, C., Braune, M., Krüger, W., Mai, H. (2024): Design of a Gust Generator for Aeroelastic Experiments in the Subsonic Wind Tunnel DNW-NWB. International Forum on Aeroelasticity and Structural Dynamics, IFASD 2024, Den Haag, The Netherlands.
https://elib.dlr.de/205804/

[38] Stalla, F., Kier, T. M., Looye, G., Michel, K., Schmidt, T.G., Hanke, C., Dillinger, J., Ritter, M., Tang, M. (2024): Wind Tunnel Testing Active Gust Load Alleviation of a Flexible Wing. International Forum on Aeroelasticity and Structural Dynamics, IFASD 2024, Den Haag, The Netherlands.
https://elib.dlr.de/205523/

[39] Abu-Zurayk, M., Merle, A., Ilic, C., Görtz, S., Schulze, M., Klimmek, T., Kaiser, C., Quero-Martin, D., Häßy, J., Becker, R.-G., Fröhler, B., Hartmann, J. (2021): Sensitivity-based Generation of Pareto Fronts for Design of Powered Aircraft Subject to a Comprehensive Set of Loads. AIAA Aviation and Aeronautics Forum and Exposition, 2021-08-02 - 2021-08-06, Washington DC / USA - Online.
https://doi.org/10.2514/6.2021-3025.

[40] Abu-Zurayk, M., Ilic, C., Schulze, M., Häßy, J., Kiehn, D., Wallace, C., Süelözgen, Ö., Kaiser, C., Dähne, S., Wegener, P., Balani, A., Reimer, L. (2024): Development of Methods for Multidisciplinary Wing Design and Optimization under Load Alleviation. Deutscher Luft- und Raumfahrtkongress, DLRK 2024, 30.9.-2.10.2024, Hamburg.